ACADEMIC PRESS

Available online at www.sciencedirect.com

SCIENCE DIRECT®

Journal of Sound and Vibration 264 (2003) 911–928

JOURNAL OF SOUND AND VIBRATION

www.elsevier.com/locate/jsvi

Active control of geometrically nonlinear transient vibration of composite plates with piezoelectric actuators

J.-X. Gao[a,*], Y.-P. Shen[b]

[a] *School of Civil Engineering, Ji-nan University, Jinan, Shandong 250022, China.*
[b] *Department of Engineering Mechanics, Xi'an Jiaotong University Xi'an, Shaanxi 710049, China.*

Received 7 March 2001; accepted 30 May 2002

Abstract

In this paper, the incremental finite element equations for geometric non-linear analysis of piezoelectric smart structures are developed using a total Lagrange approach by using virtual velocity incremental variational principles. A four-node first order shear plate element model with reduced and selective integration is also developed. Geometrically non-linear transient vibration response and control of plates with piezoelectric patches subjected to pulse loads are investigated. Active damping is introduced on the plates by coupling a self-sensing and negative velocity feedback algorithm in a closed control loop. The numerical results show that piezoelectric actuators can introduce significant damping and suppress transient vibration effectively. The effects of the number and locations of the piezoelectric actuators on the control system are also discussed.

1. Introduction

In some structures, external static and dynamic excitations can introduce large deformation or geometrical non-linearity due to small material damping or the lack of other forms of damping, especially in space. So, there is a need to investigate the induced geometrically non-linear effects on static and dynamic characteristics of structures in order to accurately design and effectively control the structural systems. In the development of intelligent structures systems, piezoelectric materials are widely used as sensors and actuators for the monitoring and control of structures and mechanical systems [1–3]. However, most of the studies on piezoelectric systems are based on

*Corresponding author. Dr. J.X Gao, Ji-nan University School of civil engineering, Jinan, Shandong 250022, China.
E-mail address: gijanxin_can@yahoo.co.uk (J.-X. Gao).

0022-460X/03/$ - see front matter
doi:10.1016/S0022-460X(02)01189-6

linear piezoelectricity and linear elasticity theories while non-linear studies of piezoelectric systems are few.

Shi and Atluri [4] presented an analytical model for active control of non-linear vibration of space structures. Pai et al. [5] developed a geometrically non-linear plate theory for the analysis of composite plates with piezoelectric layers. Yu [6] had reviewed the studies of linear and non-linear theories of elastic and piezoelectric plates. Tzou et al. [7] proposed a non-linear anisotropy piezothermoelastic shell lamination theory with application to various piezoelectric materials and studied the dynamics and control of non-linear circular plates with piezoelectric actuators. However, it becomes very difficult to solve general non-linear problems with analytical approach, and numerical calculation methods must usually be used.

Geometrically non-linear transient analysis of isotropic plates has been a subject of interest. Pica et al. [8] used Mindlin element while Akay [9] used a mixed finite element for the geometrically non-linear dynamic analysis of plates. Reddy [10] studied the geometrically non-linear transient analysis of composite plates using a finite element combining the Timoshenko-type theory and the Von-Karman plate theory. Recently, finite element models have been developed for active vibration control of linear elastic structures with piezoelectric sensors and actuators by many researchers, Tzou and Tseng [11], Ha et al. [12], Hwang and Park [13] and Gaudenzi and Bathe [14] presented a general finite element procedure which can be used to model the electro-mechanical coupled behavior of piezoelectric continua. These can also be used in a non-linear finite element analysis. The present investigation is concerned with the geometrically non-linear transient analysis and control of plates with piezoelectric sensors and actuators under applied transverse loads. In this paper, incremental finite element equations considering the geometrical non-linearity of structures with piezoelectric patches are developed based on virtual velocity incremental variational principles with the assumption of weak mechanical and electric coupling. A four-node first order shear plate element with reduced and selective integration is adopted. A self-sensing technique and velocity feedback control law are used in the active control. The transient response of plates with piezoelectric sensors and actuators subjected to transverse dynamic loading is investigated. The numerical results show that piezoelectric actuators can produce significant damping and suppress non-linear transient vibration effectively. The effects of the numbers and locations of the piezoelectric actuators on the system are also investigated.

2. Basic theory

2.1. Incremental variational principles

In an analysis dealing with both geometric and material non-linearities, an incremental solution scheme is the most suitable approach. The loading path is divided into a number of equilibrium states.

$$\Omega^{(0)}, \Omega^{(1)}, \ldots, \Omega^{(N)}, \Omega^{(N+1)}, \ldots \Omega^{(f)},$$

where, $\Omega^{(0)}$ are $\Omega^{(f)}$ the initial and final states of the deformation, respectively, $\Omega^{(N)}$ is an arbitrary intermediate state. The Green strain tensors at the $\Omega^{(N)}$ and $\Omega^{(N+1)}$ states can be expressed in terms

of the displacement and displacement increments:

$$e_{ij}(t_N) = \tfrac{1}{2}(u_{i,j} + u_{j,i} + u_{k,i}u_{k,j}), \tag{1}$$

$$e_{ij}(t_{N+1}) = \tfrac{1}{2}[(u_i + \Delta u_i)_{,j} + (u_j + \Delta u_j),_i + (u_k + \Delta u_k)_{,i}(u_k + \Delta u_k)_{,j}]. \tag{2}$$

The Green strain increment tensors take the form as

$$\Delta e_{ij} = \tfrac{1}{2}(\Delta u_{i,j} + \Delta u_{j,i} + u_{k,i}\Delta u_{k,j} + u_{k,j}\Delta u_{k,i} + \Delta u_{k,i}\Delta u_{k,j}). \tag{3}$$

Letting

$$\Delta\varepsilon_{ij} = \tfrac{1}{2}(\Delta u_{i,j} + \Delta u_{j,i} + u_{k,i}\Delta u_{k,j} + u_{k,j}\Delta u_{k,i})£\neg\Delta\eta_{ij} = \tfrac{1}{2}\Delta u_{k,i}\Delta u_{k,j}, \tag{4}$$

where $\Delta\varepsilon_{ij}$ and $\Delta\eta_{ij}$ are the linear and non linear parts of strain increment Δe_{ij}

$$\Delta e_{ij} = \Delta\varepsilon_{ij} + \Delta\eta_{ij}. \tag{5}$$

The electric field components can be conveniently expressed in term of an electric potential Φ

$$\begin{aligned} E_k &= -\Phi_{,k}, \\ E_k + \Delta E_k &= -(\Phi + \Delta\Phi)_{,k}. \end{aligned} \tag{6}$$

And the increments of the electric field are given by

$$\Delta E_k = -\Delta\Phi_{,k}. \tag{7}$$

It is possible to expand the virtual displacement principle, the virtual velocity principle and the virtual velocity increment principle to the piezoelectric continua. The virtual displacement principle including the piezoelectric effect is

$$\int_V [S_{ij}\delta e_{ij} - D_i\delta E_i]\,\mathrm{d}V = \int_V \rho_0(f_i - \ddot{u}_i)\delta u_i\,\mathrm{d}V + \int_{A_\sigma} \bar{T}_i\delta u_i\,\mathrm{d}A + \int_{A_q} \bar{Q}\delta\Phi\,\mathrm{d}A, \tag{8}$$

where S_{ij} is the Kirchhoff stress, D_i the electric displacement, f_i body force, $\bar{T}_i, \bar{Q}$ the external traction and body charge density.The virtual velocity variational principle corresponding to Eq. (8) is given by

$$\int_V [S_{ij}\delta\dot{e}_{ij} - D_i\delta\dot{E}_i]\,\mathrm{d}V = \int_V \rho_0(f_i - \ddot{u}_i)\delta\dot{u}_i\,\mathrm{d}V + \int_{A_\sigma} \bar{T}_i\delta\dot{u}_i\,\mathrm{d}A + \int_{A_q} \bar{Q}\delta\dot{\Phi}\,\mathrm{d}A. \tag{9}$$

The virtual velocity increment variational principle can be obtained through material derivative with respect to time of the Eq. (9) as follows:

$$\int_V [\dot{S}_{ij}\delta\dot{e}_{ij} + S_{ij}v_{k,i}\delta v_{k,j} - \dot{D}_i\delta\dot{E}_i]\,\mathrm{d}V = \int_V \rho_0(\dot{f}_i - \dddot{v}_i)\delta v_i\,\mathrm{d}V + \int_{A_\sigma} \dot{\bar{T}}_i\delta v_i\,\mathrm{d}A + \int_{A_q} \dot{\bar{Q}}\delta\dot{\Phi}\,\mathrm{d}A. \tag{10}$$

The increment variational principle can be further obtained using the virtual velocity increment variational principle directly:

$$\begin{aligned} &\int_V [\Delta S_{ij}\delta\Delta e_{ij} + S_{ij}\Delta u_{k,i}\delta\Delta u_{k,j} - \Delta D_i\delta\Delta E_i]\,\mathrm{d}V \\ &\quad - \left[\int_V \rho_0(\Delta f_i - \Delta\ddot{u}_i)\delta\Delta u_i\,\mathrm{d}V + \int_{A_\sigma} \Delta\bar{T}_i\delta\Delta u_i\,\mathrm{d}A + \int_{A_q} \Delta\bar{Q}\delta\Delta\Phi\,\mathrm{d}A\right] = \Delta F, \end{aligned} \tag{11}$$

where

$$\Delta F = \int_V \rho_0(f_i - \ddot{u}_i)\delta\Delta u_i \, \mathrm{d}V + \int_{A_\sigma} \bar{T}_i \delta\Delta u_i \, \mathrm{d}A + \int_{A_q} \bar{Q}\delta\Delta\Phi \, \mathrm{d}A - \int_V [S_{ij}\delta\Delta e_{ij} - D_i\delta\Delta E_i] \, \mathrm{d}V. \quad (12)$$

When the increments are assumed to be small, it is reasonable to neglect the higher order term of $\Delta S_{ij}\Delta\eta_{ij}$ in Eq. (11). Then, the total Lagrange small increment variational principle for piezoelectric systems can be expressed in the form.

$$\int_V [\Delta S_{ij}\delta\Delta\varepsilon_{ij} + S_{ij}\Delta u_{k,i}\delta\Delta u_{k,j} - \Delta D_i\delta\Delta E_i] \, \mathrm{d}V - \left[\int_V \rho_0(\Delta f_i - \Delta\ddot{u}_i)\delta\Delta u_i \, \mathrm{d}V + \int_{A_\sigma} \Delta\bar{T}_i\delta\Delta u_i \, \mathrm{d}A + \int_{A_q} \Delta\bar{Q}\delta\Delta\Phi \, \mathrm{d}A\right] = \Delta F, \quad (13)$$

$$\Delta F = \int_V \rho_0(f_i - \ddot{u}_i)\delta\Delta u_i \, \mathrm{d}V + \int_{A_\sigma} \bar{T}_i \delta\Delta u_i \, \mathrm{d}A + \int_{A_q} \bar{Q}\delta\Delta\Phi \, \mathrm{d}A - \int_V [S_{ij}\delta\Delta\varepsilon_{ij} - D_i\delta\Delta E_i] \, \mathrm{d}V, \quad (14)$$

where ΔF is the remaining term due to non-equilibrium and will be zero if it is assured that the $\Omega^{(N)}$state is in equilibrium[16]. However, the $\Omega^{(N)}$state may not be in complete equilibrium in this kind of incremental theory due to neglect of the higher order terms and computational inaccuracies. Consequently, it must retain these terms in Eq. (13) for an equilibrium check.

2.2. Constitutive equations

The incremental constitutive equations for piezoelectric continua in a Lagrange frame can be expressed by

$$[\Delta\mathbf{S}] = [\mathbf{C}][\Delta\mathbf{e}]\text{-}[\lambda][\Delta\mathbf{E}],$$
$$[\Delta\mathbf{D}] = [\boldsymbol{\lambda}]^{\mathrm{T}}[\Delta\mathbf{e}] + [\boldsymbol{\varepsilon}][\Delta\mathbf{E}], \quad (15)$$

where, $[\mathbf{C}]$ is the elastic stiffness matrix, $[\boldsymbol{\lambda}]$ is the piezoelectric constant matrix and $[\varepsilon]$ is permittivity matrix.

2.3. Finite element model and increment finite element equations

A first order shear plate theory is adopted in the finite element model presented here. The transverse shear deformation is taken into account and the shape functions only require $\mathbf{C}_0$ continuity in the model. Reduced and selective integration is used to overcome the overstiff "locking" behavior as plate is very thin. The displacements in the model can be expressed as

$$u(x, y, z, t) = u_0(x, y, t) + z\theta_y(x, y, t),$$
$$v(x, y, z, t) = v_0(x, y, t) - z\theta_x(x, y, t), \quad (16)$$
$$w(x, y, z, t) = w_0(x, y, t),$$

where u_0, v_0, w_0 are the reference surface displacements, and θ_x, θ_y are the rotational angles of the normal in the xz and yz planes, respectively.

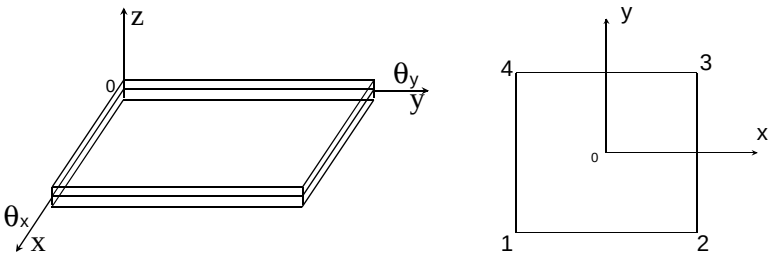

Fig. 1. A four-node isoparametric plate element.

The four-node isoparametric rectangular element with five degrees of freedom (Fig. 1) is used in the present model. The displacements on the reference surface can be expressed in term of shape functions as

$$u_0 = \sum_{i=1}^{4} N_i u_i, v_0 = \sum_{i=1}^{4} N_i v_i, w_0 = \sum_{i=1}^{4} N_i w_i, \theta_x = \sum_{i=1}^{4} N_i \theta_{xi}, \theta_y = \sum_{i=1}^{4} N_i \theta_{yi}. \tag{17}$$

Substituting into Eq. (16) yields

$$\begin{bmatrix} u \\ v \\ w \end{bmatrix} = \sum_{i=1}^{4} \begin{bmatrix} N_i & 0 & 0 & 0 & zN_i \\ 0 & N_i & 0 & -zN_i & 0 \\ 0 & 0 & N_i & 0 & 0 \end{bmatrix} \begin{Bmatrix} u_i \\ v_i \\ w_i \\ \theta_{xi} \\ \theta_{yi} \end{Bmatrix} = [N][q], \tag{18}$$

where

$$[N] = \{[N]_1, [N]_2, [N]_3, [N]_4\}, \quad [q] = \{q_1\ ,\ q_2\ ,\ q_3\ ,\ q_4\}^{\mathrm{T}},$$

$$[N]_i = \begin{bmatrix} N_i & 0 & 0 & 0 & zN_i \\ 0 & N_i & 0 & -zN_i & 0 \\ 0 & 0 & N_i & 0 & 0 \end{bmatrix}, \quad q_i = \left[u_{i,}, v_i, w_i, \theta_{xi}, \theta_{yi}\right],$$

$$N_i = \frac{1}{4}(1+\xi_0)(1+\zeta_0), \quad \xi_0 = \xi_i \xi, \quad \zeta_0 = \zeta_i \zeta, \quad i = 1, 2, 3, 4.$$

The displacement increments in the shape functions become

$$\begin{bmatrix} \Delta u \\ \Delta v \\ \Delta w \end{bmatrix} = [\mathbf{N}][\Delta \mathbf{q}], \tag{19}$$

where $[\mathbf{q}]$ and $[\Delta \mathbf{q}]$ are the generalized and incremental nodal point displacements, $[\mathbf{N}]$ the shape function matrix, ξ, ζ are the natural co-ordinates, and ξ_i, ζ_i the local co-ordinates of the nodal points.

In this paper, weak mechanical and electric coupling only is considered, in which the electric field is linear. So, it is assumed that the electric potential of every point on the surface of the

piezoelectric patch has the same value and the electric potential across the thickness of piezoelectric layer is linear variation. Then the electric potential increments become

$$\Delta\mathbf{E} = -\Delta\boldsymbol{\phi}_{,k} = -[\mathbf{A}][\Delta\boldsymbol{\phi}],$$
$$[\mathbf{A}] = \left[\frac{\partial}{\partial x}\ \frac{\partial}{\partial y}\ \frac{\partial}{\partial z}\right]^{\mathrm{T}} = \left[0 \quad 0 \quad \frac{1}{H}\right]^{\mathrm{T}}, \tag{20}$$

where H is the thickness of the piezoelectric patch. Substituting Eq. (19) into Eq. (5) yields

$$[\Delta\mathbf{e}] = \Delta\boldsymbol{\varepsilon}_{ij} + \Delta\boldsymbol{\eta}_{ij} = \left\{[\mathbf{B}]_L + [\mathbf{B}]_{NL}\right\}\{\Delta\mathbf{q}\} = [\mathbf{B}][\Delta\mathbf{q}], \tag{21}$$

where $[\mathbf{B}]_L$, $[\mathbf{B}]_{NL}$ are the linear and non-linear parts of incremental strain–displacement matrix respectively. Substituting Eqs. (15), (19)–(21) into the total Lagrange small increment variational principle, the left part of Eq. (13) will be

$$\begin{aligned}\int_V \Delta S_{ij}\delta\Delta e_{ij}\,\mathrm{d}V &= \int_V \{\delta\Delta e\}^{\mathrm{T}}[\Delta S]\,\mathrm{d}V \\ &= \int_V \{\delta\Delta\mathbf{q}\}^{\mathrm{T}}\left\{[\mathbf{B}]_L + [\mathbf{B}]_{NL}\right\}^{\mathrm{T}}\left\{[\mathbf{C}]\left[[\mathbf{B}]_L + [\mathbf{B}]_{NL}\right]\{\delta\mathbf{q}\} + [\boldsymbol{\lambda}][\mathbf{A}]\{\Delta\boldsymbol{\phi}\}\right\}\mathrm{d}V \\ &= \{\delta\Delta\mathbf{q}\}^{\mathrm{T}}\int_V \{[\mathbf{B}]_L^{\mathrm{T}}[\mathbf{C}][\mathbf{B}]_L + [\mathbf{B}]_L^{\mathrm{T}}[\mathbf{C}][\mathbf{B}]_{NL} + [\mathbf{B}]_{NL}^{\mathrm{T}}[\mathbf{C}][\mathbf{B}]_L \\ &\quad + [\mathbf{B}]_{NL}^{\mathrm{T}}[\mathbf{C}][\mathbf{B}]_{NL}\}\{\Delta\mathbf{q}\}\,\mathrm{d}V + \{\delta\Delta\mathbf{q}\}^{\mathrm{T}}\int_V \left\{[\mathbf{B}]_L^{\mathrm{T}}[\boldsymbol{\lambda}][\mathbf{A}] + [\mathbf{B}]_{NL}^{\mathrm{T}}[\boldsymbol{\lambda}][\mathbf{A}]\right\}\{\Delta\boldsymbol{\phi}\}\,\mathrm{d}V,\end{aligned} \tag{22}$$

$$\int_V S_{ij}\Delta u_{k,i}\delta\Delta u_{k,j}\,\mathrm{d}V = \{\Delta\mathbf{q}\}^{\mathrm{T}}\int_V \left[\frac{\partial\mathbf{N}}{\partial X}\right]^{\mathrm{T}}[\mathbf{S}]\left[\frac{\partial\mathbf{N}}{\partial X}\right]\{\Delta\mathbf{q}\}\,\mathrm{d}V, \tag{23}$$

$$\begin{aligned}\int_V \Delta D_i\delta\Delta\mathbf{E}_i\,\mathrm{d}V &= \int_V [\delta\Delta\mathbf{E}]^{\mathrm{T}}[\Delta\mathbf{D}]\,\mathrm{d}V \\ &= -\{\delta\Delta\boldsymbol{\phi}\}^{\mathrm{T}}\int_V \left\{[\mathbf{A}]^{\mathrm{T}}[\boldsymbol{\lambda}]^{\mathrm{T}}[\mathbf{B}]_L + [\mathbf{A}]^{\mathrm{T}}[\boldsymbol{\lambda}]^{\mathrm{T}}[\mathbf{B}]_{NL}\right\}\{\Delta\mathbf{q}\} - [\mathbf{A}]^{\mathrm{T}}[\boldsymbol{\varepsilon}][\mathbf{A}]\{\Delta\boldsymbol{\phi}\}\}\,\mathrm{d}V,\end{aligned} \tag{24}$$

$$\begin{aligned}&\int_V \rho_0(\Delta f_i - \Delta\ddot{u})\delta u_i\,\mathrm{d}V + \int_{A_\sigma}\Delta\bar{T}_i\delta\Delta u_i\,\mathrm{d}A + \int_{A_q}\Delta\bar{Q}\delta\Delta\Phi\,\mathrm{d}A] \\ &\quad = \{\delta\Delta\mathbf{q}\}^{\mathrm{T}}\left\{\int_V \rho_o\{[\mathbf{N}]^{\mathrm{T}}[\Delta\mathbf{f}] - [\mathbf{N}]^{\mathrm{T}}[\mathbf{N}][\Delta\ddot{\mathbf{q}}]\}\,\mathrm{d}V + \int_{A\sigma}[\mathbf{N}][\Delta\bar{T}]\,\mathrm{d}A\right\} \\ &\qquad + \{\delta\Delta\boldsymbol{\phi}\}^{\mathrm{T}}\int_{A_Q}[\mathbf{A}]^{\mathrm{T}}[\Delta\bar{\mathbf{Q}}]\,\mathrm{d}A.\end{aligned} \tag{25}$$

The right part of Eq. (13) will be

$$\begin{aligned}\Delta\mathbf{F} = \{\delta\Delta\mathbf{q}\}^{\mathrm{T}}&\left\{\int_V \rho_0\left\{[\mathbf{N}]^{\mathrm{T}}[\mathbf{f}] - [\mathbf{N}]^{\mathrm{T}}[\mathbf{N}][\ddot{\mathbf{q}}]\right\}\mathrm{d}V + \int_{A_\sigma}[\mathbf{N}]^{\mathrm{T}}[\bar{T}]\,\mathrm{d}A\right. \\ &\left. - \int_V [\mathbf{B}]^{\mathrm{T}}[\mathbf{S}]\,\mathrm{d}V\right\} + \{\delta\Delta\boldsymbol{\phi}\}^{\mathrm{T}}\left\{\int_{A_\sigma}[\mathbf{A}]^{\mathrm{T}}[\bar{\mathbf{Q}}]\,\mathrm{d}A + \int_V [\mathbf{A}]^{\mathrm{T}}[\mathbf{D}]\,\mathrm{d}V\right\}.\end{aligned} \tag{26}$$

Rearranging the above equations, the increment finite element dynamic equations can be written as

$$\left\{[\mathbf{M}]\Delta\ddot{\mathbf{q}} + \left\{[\mathbf{K}]_L + [\mathbf{K}]_{NL} + [\mathbf{K}]_\sigma\right\}\Delta\mathbf{q} + \left\{[\mathbf{K}]_{\phi L} + [\mathbf{K}]_{\phi NL}\right\}\Delta\boldsymbol{\phi} = \Delta\mathbf{F}_1 + \Delta\mathbf{F}_2 + \Delta\mathbf{P}_1,\right.$$

$$\left\{[\mathbf{K}]_{qL} + [\mathbf{K}]_{qNL}\right\}\Delta\mathbf{q} - [\mathbf{K}]_{\phi\phi}\Delta\boldsymbol{\phi} = \Delta\mathbf{F}_3 + \Delta\mathbf{P}_2, \tag{27}$$

where

$$[\mathbf{M}] = \int_V \rho_0[\mathbf{N}]^{\mathrm{T}}[\mathbf{N}]\,\mathrm{d}V, \qquad [\mathbf{K}]_L = \int_V [\mathbf{B}]_L^{\mathrm{T}}[\mathbf{C}][\mathbf{B}]_L\,\mathrm{d}V,$$

$$[\mathbf{K}]_{NL} = \int_V \{[\mathbf{B}]_L^{\mathrm{T}}[\mathbf{C}][\mathbf{B}]_{NL} + [\mathbf{B}]_{NL}^{\mathrm{T}}[\mathbf{C}][\mathbf{B}]_L + [\mathbf{B}]_{NL}^{\mathrm{T}}[\mathbf{C}][\mathbf{B}]_{NL}\}\,\mathrm{d}V, \tag{28}$$

$$[\mathbf{K}]_\sigma = \int_V \left[\frac{\partial\mathbf{N}}{\partial X}\right]^{\mathrm{T}}[\mathbf{S}]\left[\frac{\partial\mathbf{N}}{\partial X}\right]\,\mathrm{d}V,$$

$$[\mathbf{K}]_{\phi l} = \int_V [\mathbf{B}]_L^{\mathrm{T}}[\boldsymbol{\lambda}][\mathbf{A}]\,\mathrm{d}V, \quad [\mathbf{k}]_{ql} = \int_V [\mathbf{A}]^{\mathrm{T}}[\boldsymbol{\lambda}]^{\mathrm{T}}[\mathbf{B}]_L\,\mathrm{d}V,$$

$$[\mathbf{k}]_{\phi Nl} = \int_V [\mathbf{B}]_{NL}^{\mathrm{T}}[\boldsymbol{\lambda}][\mathbf{A}]\,\mathrm{d}V, \quad [\mathbf{k}]_{qNL} = \int_V [\mathbf{A}]^{\mathrm{T}}[\boldsymbol{\lambda}]^{\mathrm{T}}[\mathbf{B}]_{NL}\,\mathrm{d}V,$$

$$[\mathbf{k}]_{\phi\phi} = \int_V [\mathbf{A}]^{\mathrm{T}}[\boldsymbol{\varepsilon}][\mathbf{A}]\,\mathrm{d}V, \quad \Delta\mathbf{F}_1 = \int_{A_\sigma} [\mathbf{N}]^{\mathrm{T}}[\Delta\bar{\mathbf{T}}]\,\mathrm{d}A,$$

$$\Delta\mathbf{F}_2 = \int_V \rho_0[\mathbf{N}]^{\mathrm{T}}[\Delta\mathbf{f}]\,\mathrm{d}V, \quad \Delta\mathbf{F}_3 = -\int_{A_q} [\mathbf{A}]^{\mathrm{T}}[\Delta\bar{\mathbf{Q}}]\,\mathrm{d}A,$$

$$\Delta P_1 = \int_V \rho_0\{[\mathbf{N}]^{\mathrm{T}}[\mathbf{f}] - [\mathbf{N}]^{\mathrm{T}}[\mathbf{N}][\ddot{\mathbf{q}}]\}\,\mathrm{d}V + \int_{A_\sigma} [\mathbf{N}]^{\mathrm{T}}[\bar{\mathbf{T}}]\,\mathrm{d}A - \int_V [\mathbf{B}]^{\mathrm{T}}[\mathbf{S}]\,\mathrm{d}V,$$

$$\Delta P_2 = -\int_{A_\sigma} [\mathbf{A}]^{\mathrm{T}}[\bar{\mathbf{Q}}]\mathrm{d}A + \int_V [\mathbf{A}]^{\mathrm{T}}[\mathbf{D}]\,\mathrm{d}V.$$

In the case of small increment,

$$[\mathbf{K}]_{NL} = [\mathbf{K}]_{\phi NL} = [\mathbf{K}]_{qNL} \approx \mathbf{0}, \tag{29}$$

$$[\mathbf{B}] = [\mathbf{B}]_L = [[\mathbf{B}]_1\ [\mathbf{B}]_2\ [\mathbf{B}]_3\ [\mathbf{B}]_4], \tag{30}$$

where

$$[\mathbf{B}]_i = \begin{bmatrix} \left(1+\frac{\partial u}{\partial x}\right)\frac{\partial N_i}{\partial x} & \frac{\partial v}{\partial x}\frac{\partial N_i}{\partial x} & \frac{\partial w}{\partial x}\frac{\partial N_i}{\partial x} & -z\frac{\partial v}{\partial x}\frac{\partial N_i}{\partial x} & z\left(1+\frac{\partial u}{\partial x}\right)\frac{\partial N_i}{\partial x} \\ \frac{\partial u}{\partial y}\frac{\partial N_i}{\partial y} & \left(1+\frac{\partial v}{\partial y}\right)\frac{\partial N_i}{\partial y} & \frac{\partial w}{\partial y}\frac{\partial N_i}{\partial y} & -z\left(1+\frac{\partial v}{\partial y}\right)\frac{\partial N_i}{\partial y} & z\frac{\partial u}{\partial y}\frac{\partial N_i}{\partial y} \\ \left(1+\frac{\partial u}{\partial x}\right)\frac{\partial N_i}{\partial y}+\frac{\partial u}{\partial y}\frac{\partial N_i}{\partial x} & \left(1+\frac{\partial v}{\partial y}\right)\frac{\partial N_i}{\partial x}+\frac{\partial v}{\partial x}\frac{\partial N_i}{\partial y} & \frac{\partial w}{\partial y}\frac{\partial N_i}{\partial x}+\frac{\partial w}{\partial x}\frac{\partial N_i}{\partial y} & -z\left[\left(1+\frac{\partial v}{\partial y}\right)\frac{\partial N_i}{\partial x}+\frac{\partial v}{\partial x}\frac{\partial N_i}{\partial y}\right] & z\left[\left(1+\frac{\partial u}{\partial x}\right)\frac{\partial N_i}{\partial y}+\frac{\partial u}{\partial y}\frac{\partial N_i}{\partial x}\right] \\ \frac{\partial u}{\partial z}\frac{\partial N_i}{\partial y} & \frac{\partial v}{\partial z}\frac{\partial N_i}{\partial y} & \frac{\partial N_i}{\partial y} & -\left(1+\frac{\partial v}{\partial y}\right)N_i - z\frac{\partial u}{\partial y}\frac{\partial N_i}{\partial y} & \frac{\partial u}{\partial y}N_i + z\frac{\partial u}{\partial z}\frac{\partial N_i}{\partial y} \\ \frac{\partial u}{\partial z}\frac{\partial N_i}{\partial x} & \frac{\partial v}{\partial z}\frac{\partial N_i}{\partial x} & \frac{\partial N_i}{\partial x} & -z\frac{\partial v}{\partial z}\frac{\partial N_i}{\partial x}-\frac{\partial v}{\partial x}N_i & \left(1+\frac{\partial u}{\partial x}\right)N_i + z\frac{\partial u}{\partial z}\frac{\partial N_i}{\partial x} \end{bmatrix}.$$

The following derivation is based on the small increment condition.

2.4. Active control algorithm

Yellin and Shen [17] introduced the self-sensing technique into active control. In the self-sensing algorithm, the piezoelectric patch is used simultaneously as both a sensor and an actuator. Therefore, the sensor and actuator are truly collocated. Apart from the better stability, the self-sensing algorithm has many other desirable features, such as simplicity, practicality and reducing weight penalty.

The self-sensing technique is employed in this paper. The sensed voltage can be obtained from the second equation of Eq. (27)

$$[\Delta\boldsymbol{\phi}] = \alpha[\mathbf{K}]_{\phi\phi}^{-1}[\mathbf{K}]_{qL}[\Delta\mathbf{q}], \tag{31}$$

where α is a self-sensing constant obtained from the self-sensing bridge circuit [16].

The velocity feedback control law is adopted in this paper and the feedback actuating electric field takes the forms

$$\begin{aligned} [\Delta\boldsymbol{\phi}] &= -G_c[\Delta\dot{\boldsymbol{\phi}}] = -G[\mathbf{K}]_{\phi\phi}^{-1}[\mathbf{K}]_{qL}[\Delta\dot{\mathbf{q}}], \\ G &= G_c\alpha, \end{aligned} \tag{32}$$

where, G_c is the gain of feedback control and G is active control gain. Substituting Eqs. (29) and (32) into Eq. (27), the system equation of motion takes the final form

$$[\mathbf{M}]\Delta\ddot{\mathbf{q}} + [\mathbf{C}]\Delta\dot{\mathbf{q}} + [\mathbf{K}]\Delta\mathbf{q} = \mathbf{F}, \tag{33}$$

where

$$[\mathbf{C}] = G[\mathbf{K}]_{\phi L}[\mathbf{K}]_{\phi\phi}^{-1}[\mathbf{K}]_{qL}, \quad [\mathbf{K}] = [\mathbf{K}]_L + [\mathbf{K}]_\sigma, \quad \mathbf{F} = \Delta\mathbf{F}_1 + \Delta\mathbf{F}_2 + \Delta\mathbf{P}_1.$$

2.5. Solution algorithms

The Newmark method is used to solve Eq. (33), and the solution at the end of a time step Δt are expressed as follows:

$$\begin{aligned} \dot{\mathbf{q}}_{t+\Delta t=} &= \dot{\mathbf{q}}_t + [(1-\beta)\ddot{\mathbf{q}}_t + \beta\ddot{\mathbf{q}}_{t+\Delta t}]\Delta t, \\ \mathbf{q}_{t+\Delta t=} &= \mathbf{q}_t + \dot{\mathbf{q}}_t\Delta t + [(\tfrac{1}{2}-\alpha)\ddot{\mathbf{q}}_t + \alpha\ddot{\mathbf{q}}_{t+\Delta t}]\Delta t^2 \end{aligned} \tag{34}$$

and rearranging Eq. (34) obtains

$$\ddot{\mathbf{q}}_{t+\Delta t} = \frac{1}{\alpha \Delta t^2}(\mathbf{q}_{t+\Delta t} - \mathbf{q}_t) - \frac{1}{\alpha \Delta t}\dot{\mathbf{q}}_t - \left(\frac{1}{2\alpha} - 1\right)\ddot{\mathbf{q}}_t,$$

$$\Delta \ddot{\mathbf{q}} = \ddot{\mathbf{q}}_{t+\Delta t} - \ddot{\mathbf{q}}_t = \frac{1}{\alpha \Delta t^2}\Delta \mathbf{q} - \frac{1}{\alpha \Delta t}\dot{\mathbf{q}}_t - \frac{1}{2\alpha}\ddot{\mathbf{q}}_t$$

$$\Delta \dot{\mathbf{q}} = \dot{\mathbf{q}}_{t+\Delta t} - \dot{\mathbf{q}}_t = [(1-\beta)\ddot{\mathbf{q}}_t + \beta \ddot{\mathbf{q}}_{t+\Delta t}]\Delta t = [\ddot{\mathbf{q}}_t + \beta(\ddot{\mathbf{q}}_{t+\Delta t} - \ddot{\mathbf{q}}_t)]\Delta t$$

$$= \frac{\beta}{\alpha \Delta t}\Delta \mathbf{q} - \frac{\beta}{\alpha}\dot{\mathbf{q}}_t + \left(1 - \frac{\beta}{2\alpha}\right)\ddot{\mathbf{q}}_t \Delta t. \tag{35}$$

Substituting Eq. (35) into Eq. (33) yields

$$c_0 = \frac{1}{\alpha \Delta t^2}, \quad c_1 = \frac{\beta}{\alpha \Delta t}, \quad c_2 = \frac{1}{\alpha \Delta t}, \quad c_3 = \frac{1}{2\alpha} - 1, \quad c_4 = \frac{\beta}{\alpha}, \quad c_5 = \left(\frac{\beta}{2\alpha} - 1\right)\Delta t,$$

$$c_6 = (1-\beta)\Delta t, \quad c_7 = \beta \Delta t,$$

$$[c_0\mathbf{M} + c_1\mathbf{C} + \mathbf{K}]\Delta \mathbf{q} = \mathbf{F} + \mathbf{M}[c_2\dot{\mathbf{q}}_t + (c_3+1)\ddot{\mathbf{q}}_t] + \mathbf{C}[c_4\dot{\mathbf{q}}_t + c_5\ddot{\mathbf{q}}_t]. \tag{36}$$

Once the solution $\Delta \mathbf{q}$ is known, the velocity and accelerations can be obtained from

$$\ddot{\mathbf{q}}_{t+\Delta t} = c_0 \Delta \mathbf{q} - c_2\dot{\mathbf{q}}_t - c_3\ddot{\mathbf{q}}_t, \quad \dot{\mathbf{q}}_{t+\Delta t} = \dot{\mathbf{q}}_t + c_6\ddot{\mathbf{q}}_t + c_7\ddot{\mathbf{q}}_{t+\Delta t}. \tag{37}$$

3. Numerical examples and discussion

First, in order to prove the validity of the formulations and related finite element codes presented in this paper, a simply supported plate under a uniform pulse loading is analyzed and the results obtained are compared with those in the literature. A thin square plate with the following parameters is considered (see Fig. 2 and Ref. [9]).

$$a = 2.438 \text{ m}, \quad h = 6.35 \text{ mm}, \quad v = 0.25, \quad E = 68.9 \text{ Gpa}, \quad \rho = 2.5 \times 10^3 \text{ Kg/m}^3,$$

$$q(x, y, t) = 47.84 \text{ N/m}^2, \quad 0 \leqslant t < \infty.$$

The same plate was analyzed by Akay [9] who developed a mixed finite element and employed 6×6 mesh and a time increment of $\Delta t = 0.005$ s. In the present calculation, an (8×8) mesh and a time increment of $\Delta t = 0.005$ s, and the constant average acceleration method with $\alpha = 0.25$, $\beta = 0.5$

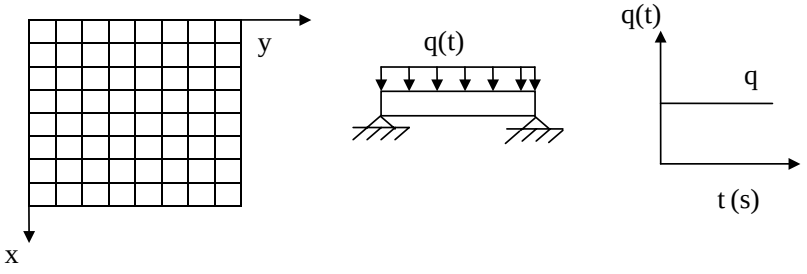

Fig. 2. A simply supported square plate under a uniform pulse loading.

in the Newmark method are adopted. The center deflection of the plate obtained within 0.5 s. is presented in Fig. 3. The center deflections of the present calculation, as well as Akay's are plotted in Fig. 4, and one can see that there is a good agreement in the results.

In order to verify the formulations as piezoelectric effects is taken into account, a cantilevered piezoelectric bimorph beam [15] with two identical PVDF films is considered, and the material properties are shown in Table 1.

When 1 V external voltage is applied to the PVDF films with opposite polarities, the induced strain generates moment that bends the beam, and the deflection of the beam can be calculated by

$$u(x) = 1.5\,\frac{d_{31}V}{E}\,\left(\frac{x}{h}\right)^2.$$

The present finite element results and analytical deflection are shown in Fig. 5 and there is a good agreement between the results.

The output voltage due to the direct piezoelectric effect is also investigated. When the tip deflection of the pure bending bimorph beam equals h_d, the analytical sensed voltage can be

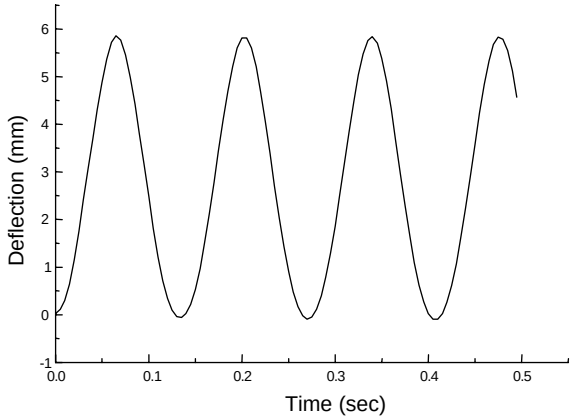

Fig. 3. Central deflection values of nonlinear dynamic response.

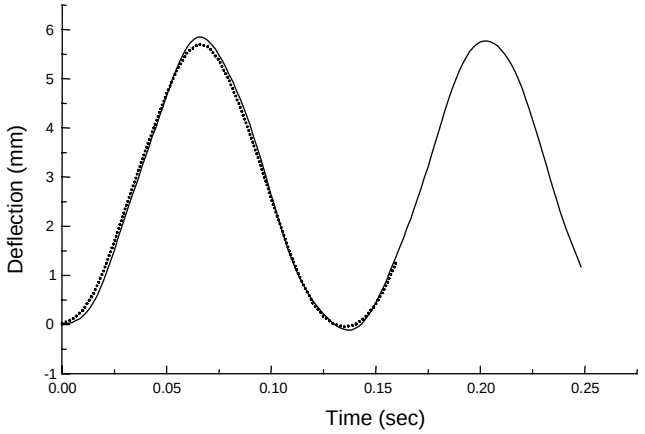

Fig. 4. Solution comparison: ——, present solution; ……, solution in Ref. [9].

Table 1
The material properties of the PVDF and the elastic beam

	E (N/m^2)	v	ρ (kg/m^3)	h (mm)	l (mm)	d_{31} (C/N)	ε_{33} (F/m)
PVDF	2.0E9	0.29	1800	1.0	100	2.2E−11	1.062E−10

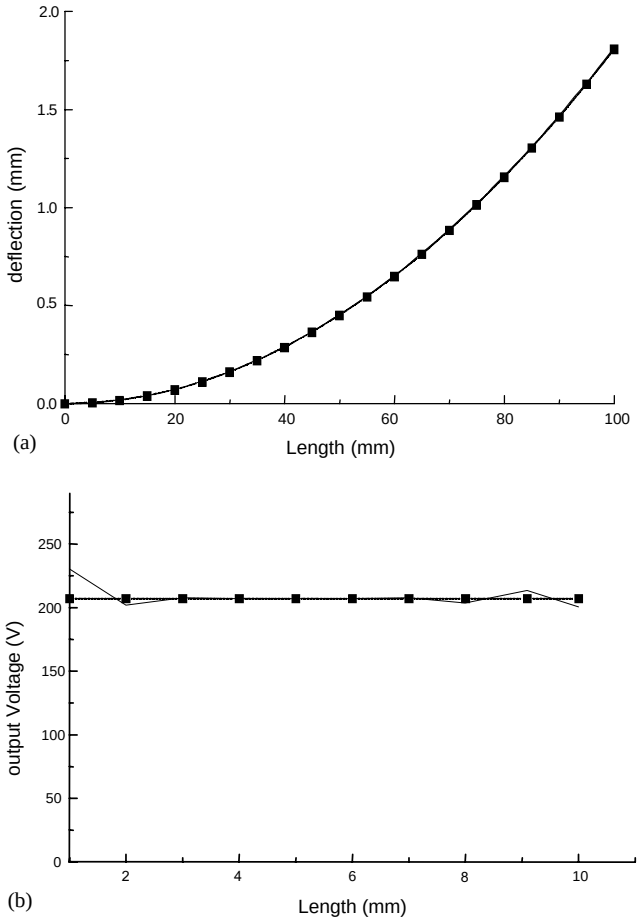

Fig. 5. Direct and inverse piezoelectric effects of Bimorph beam: ——, FEM solution; ……, analytic solution.

obtained from

$$\phi_s = \frac{2d_{31}Eh^2h_d}{\varepsilon_{33}l^2},$$

where E is Young's modulus, and l the length of piezoelectric bimorph beam. The output voltages of the sensors calculated by the present work are compared with those from above equation in Fig. 5(b) as h_d is 1 cm. The present results show good agreement with the analytical solution. Thus, both the present formulations and code are verified numerically.

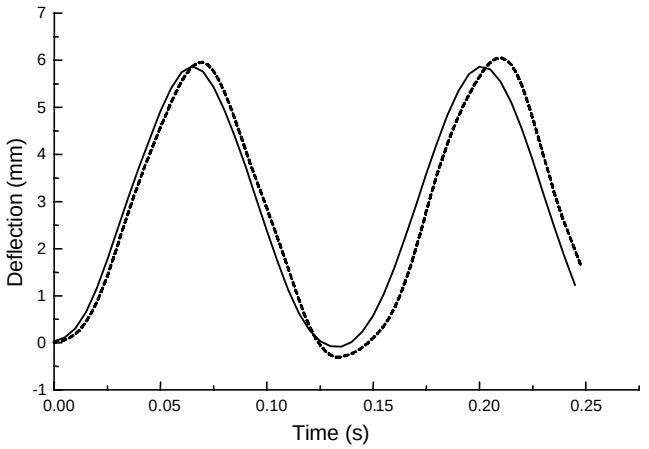

Fig. 6. Comparisons between lumped and consistent matrices: ——, consistent mass matrix; ……, lumped mass matrix.

In the finite element analysis, there are usually two kinds of approaches to treat element mass, i.e., consistent mass matrix and lumped mass matrix. The consistent mass matrix is defined by Eq. (28), while the lumped mass matrix is a diagonal matrix based on the assumption that the element mass is lumped on the element nodes. So, the lumped mass matrix is a simplified calculation. The comparison between lumped and consistent matrices is presented in Fig. 6. The results show that the difference between the two kinds of mass matrices is not very large. The consistent mass matrix is used in following calculations.

3.1. The linear and non-linear dynamic responses

The natural frequencies of the plate under the linear small deflection condition can be obtained with equation

$$\omega_{ij} = \frac{\pi^2(i^{2+} + j^2)}{a^2}\sqrt{\frac{D_0}{\rho h}}.$$

For the system here, the first modal frequency is $\omega_{11} = 33$ rad/s, and the cycle $T = 0.19$ s.

The second modal frequency is $\omega_{12} = 82.5$ rad/s, and the cycle $T = 0.076$ s.

The linear and non-linear transient dynamic responses of the plate under a suddenly applied uniform pulse load are shown in Fig. 7(a). It is observed that the linear and non-linear transient dynamic responses are quite different. In the case of linearity, the plate will vibrate in its first modal frequency, while in the non-linear case the response frequency will change with the values of the load. The plots of center deflection versus time in the non-linear and linear cases under various loads are shown in Figs. 8(a) and (b). One can notice that the response period of the center deflection decreases with increasing values of the load in the non-linear case, while keeping constant in the linear case. The results of the present non-linear analysis agree closely with the results of Akay. The linear and non-linear transient responses will approach gradually with the decrease of the load as shown in Fig. 7 (b), in which the load is one tenth of the original load ($q = q(x, y, t/10)$.

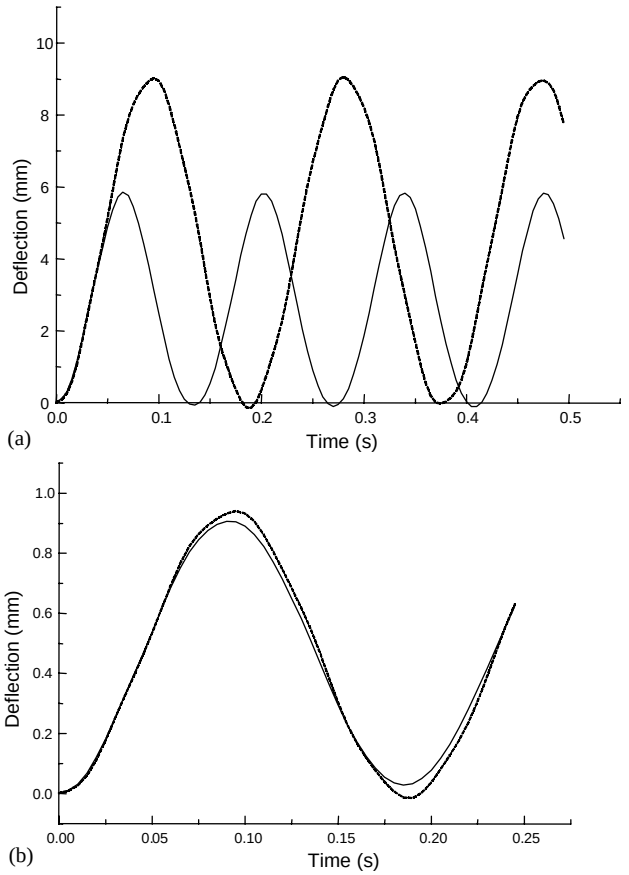

Fig. 7. Linear and non-linear responses with a pulse load: ——, linearity; ……, non-linearity.

3.2. *The influence of the piezoelectric patches*

Piezoelectric film PVDF and piezoceramics PZT-5 are used and the material properties are shown in Tables 1 and 2.

Proper selection of the number and location of the piezoelectric sensors/actuators is critical to control structural vibration efficiently. Several piezoelectric patches and locations, as shown in Fig. 9, are selected to control the plate deformation in this paper. Fig. 10 shows that the influence of the mass and stiffness of the piezoelectric patches on the dynamic response is obvious as only one patch is pasted on the plate, as shown in Fig. 9(a), and piezoelectric PVDF, ceramics PZT-5 are used, respectively. The influence will be more evident if more piezoelectric patches are pasted.

3.3. *Active vibration suppression for the transient response*

The active control effects on transient vibration are shown in Fig. 11 as one piezoelectric patches is used, as shown in Fig. 9(a), and control gains are 0, 0.01, 0.05, 0.1, respectively. The effect of active control with one actuator is obvious.

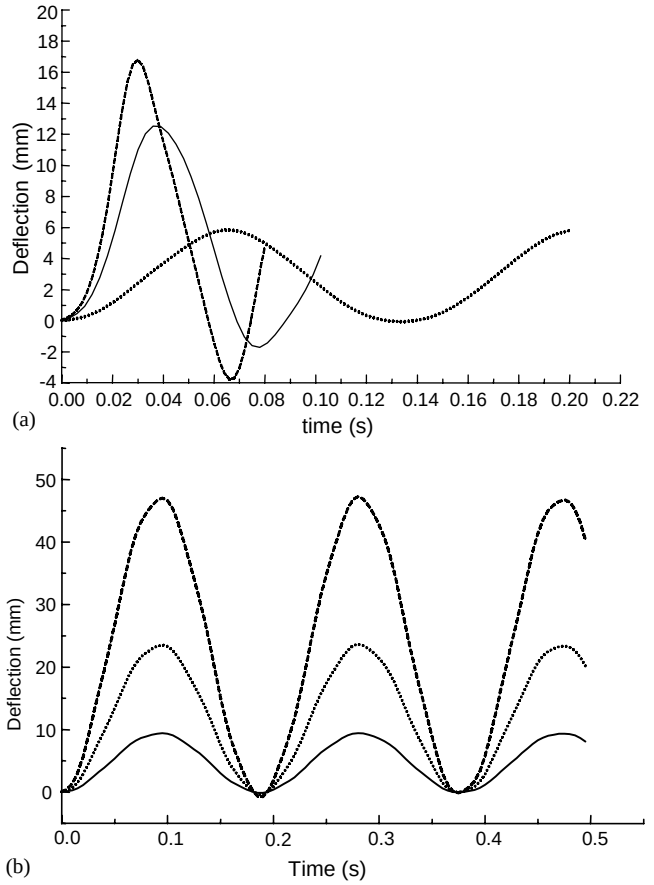

Fig. 8. (a) Non-linear responses versus different loads: …… q, —— $5q$, …… $10q$. (b) Linear responses versus different loads: —— q, …… $2.5q$, — — — — $5q$.

Table 2
The material properties of the PZT-5

	E (N/m^2)	v	ρ (kg/m^3)	h (mm)	l (mm)	d_{31} (C/N)	ε_{33} (F/m)
PZT-5	49E9	0.3	7800	1.0		−12.1E−11	1.3E−8

Fig. 12 illustrates the actuation ability of active control on the transient response with four piezoelectric actuators, as shown in Fig. 9(b), and control gains are 0.01,0.05,0.1, respectively. It is clearly shown that the numbers of actuators and control gains have a significant effect on the control of the transient vibration. The vibration introduced by a pulse load has nearly died out within 1 s as shown in Fig. 12(c).

It can be seen from Fig. 13 that the locations of the piezoelectric actuators have a significant effect on the control of the deflection, where four actuators are patched on plate as shown in Fig. 9(c) and 9(d), and the control gain is 0.1. It is also clearly shown that there is a better actuation ability as the actuators are closer to the center of the plate.

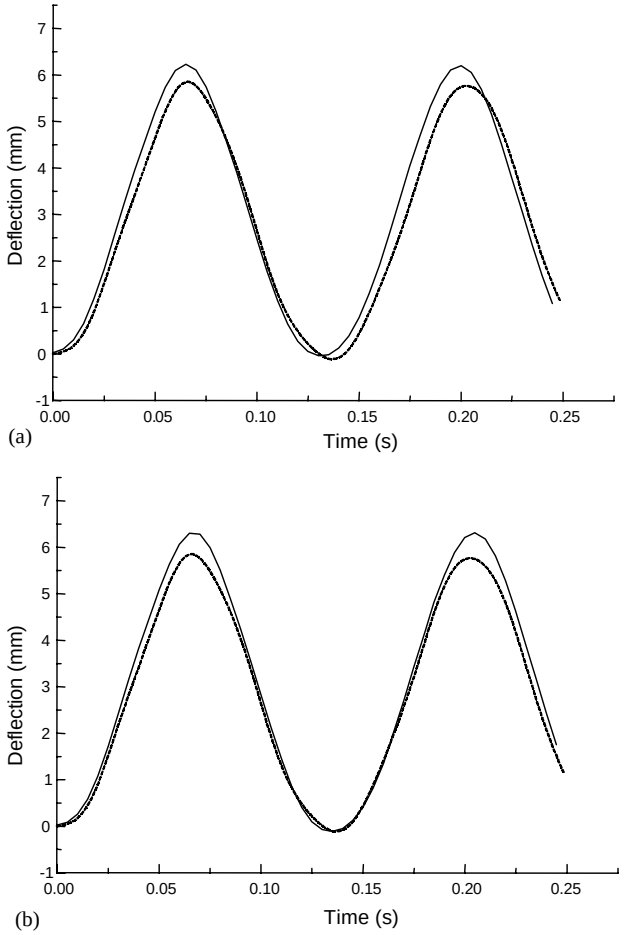

Fig. 9. The effects of mass and stiff of piezoelectric patch on calculations: (a) ——, with PVDF piezoelectric patch; ....., without PVDF piezoelectric patch; (b) ——, with PZT piezoelectric patch; ....., without PZT piezoelectric patch.

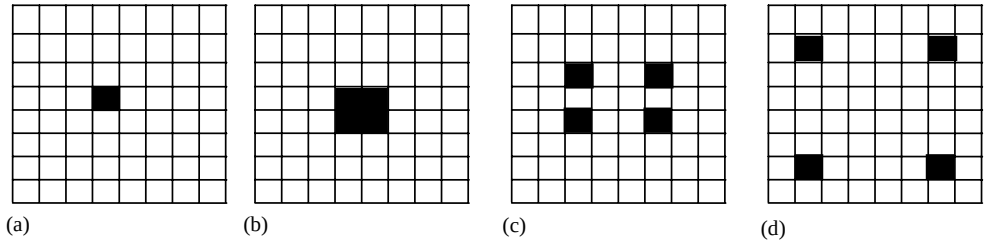

Fig. 10. The number and locations of piezoelectric patches.

4. Conclusions

Based on a total Lagrange approach and first order shear plate theory, an incremental non-linear finite element model for the active vibration control of a plate with piezoelectric patches is

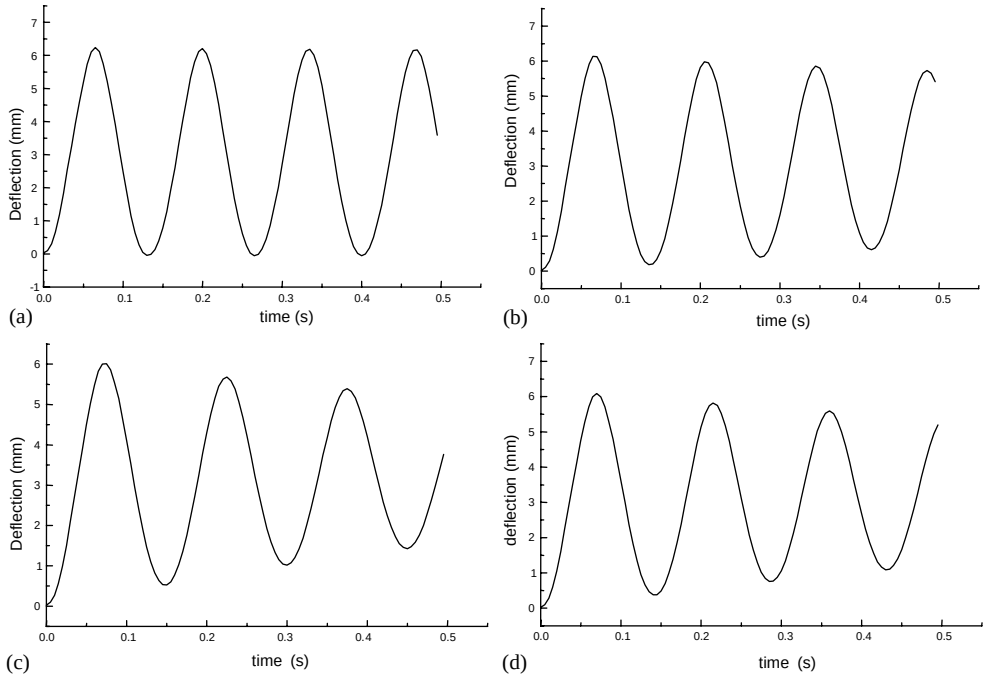

Fig. 11. Actuation ability of active control with one actuator: (a) control gain $G = 0$; (b) $G = 0.01$; (c) $G = 0.05$; (d) $G = 0.1$.

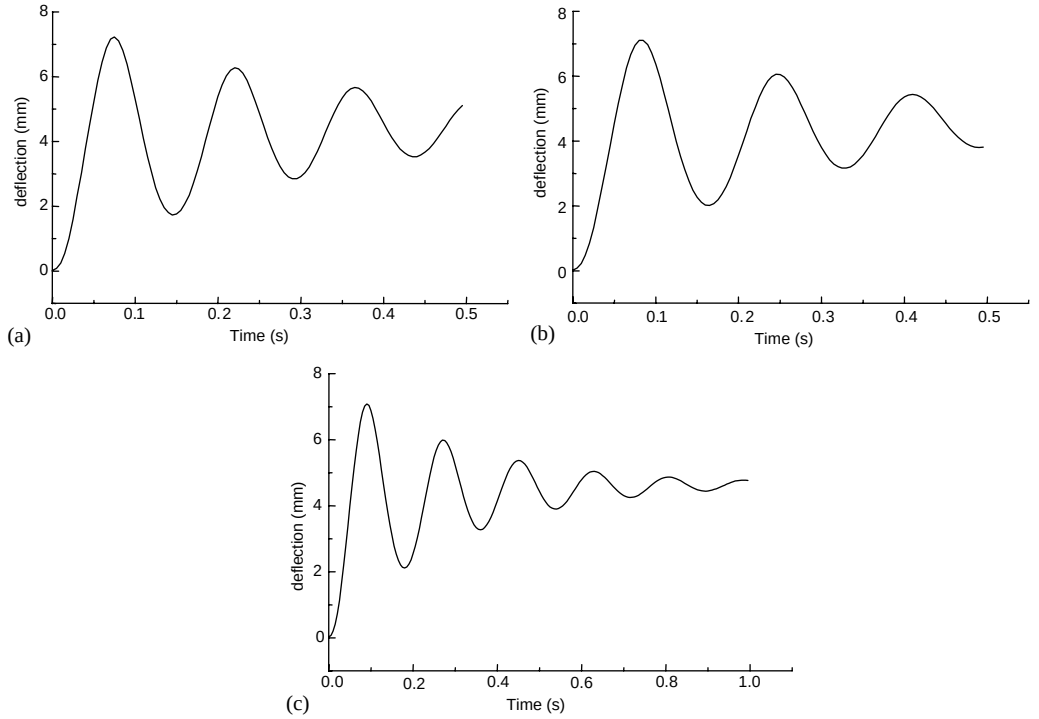

Fig. 12. Actuation ability of active control with four actuators: (a) control gain $G = 0.01$; (b) $G = 0.05$; (c) $G = 0.1$.

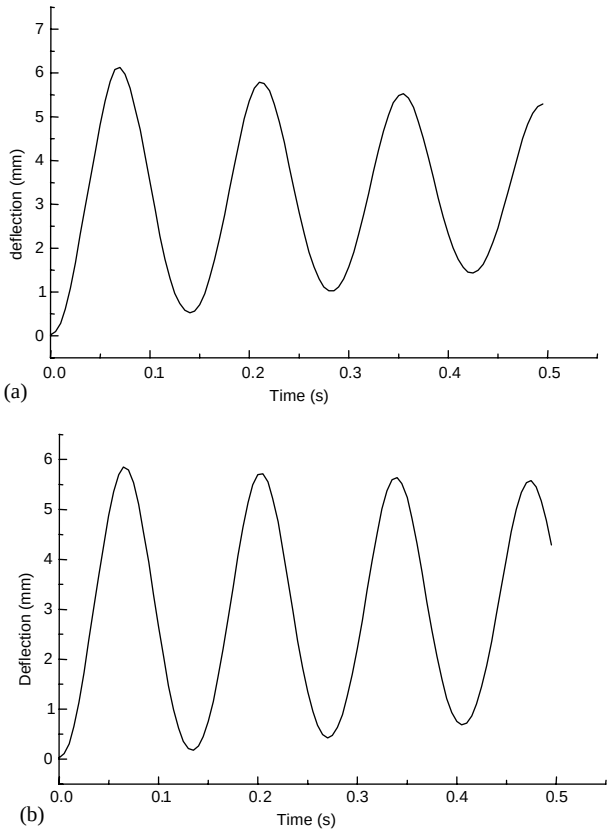

Fig. 13. The actuation ability with different locations of actuators: (a) actuator' locations as shown in Fig. 10(c); (b) actuator' locations as shown in Fig. 10(d).

developed by using virtual velocity incremental variation principles. A self-sensing and negative velocity feedback algorithm is introduced in a closed control loop. The results show that the finite element model of a four-node rectangular element with five degrees of freedom is efficient and accurate. It can be effective for thin and thick plate since reduced and selective integration is used. At the same time, the transverse shear deformation is taken into account and C_0 continuity is only required in the model. The numerical results show that piezoelectric actuators can produce significant damping and suppress transient vibration effectively, and the numbers and locations of the piezoelectric actuators have critical influence on both the shape control and the vibration suppression of the structures.

References

[1] D.E. Crawly, J. Luis, Use of piezoelectric actuators as elements of intelligent structure, American Institute of Aeronautics and Astronautics Journal 25 (10) (1987) 1373–1385.

[2] C.R. Fuller, C.H. Hansen, S. D, Snyder active control of sound radiation from a vibrating rectangular panel by sound sources and vibration inputs: an experimental comparison, Journal of Sound and Vibration 145, (1991) 195–215.
[3] A. Baz, American Society of Mechanical Engineers Boundary control of beams using active constrained layer damping, Journal of Vibration and Acoustics 119 (1997) 166–172.
[4] G. Shi, S.N. Atluri, Active control of nonlinear dynamic response of space-frames using piezoelectric actuators, Computers and Structures 34 (4) (1990) 549–564.
[5] P.F. Pai, A.H. Nayfeh, K. Oh, D.T. Mook, A refined nonlinear model of composite plates with integrated piezoelectric actuators and sensors, International Journal of Solids and Structures 30 (12) (1993) 1603–1630.
[6] Y.Y. Yu, On the ordinary, generalized, and pseudo-variational equations of motion in nonlinear elasticity, piezoelectricity, and classical plate theory, American Society of Mechanical Engineers Journal of Applied Mechanics 62 (1995) 471–478.
[7] H.S. Tzou, Nonlinear piezothermoelasticity and multi-field actuation, Part1 Part2, American Society of Mechanical Engineers Journal of Applied Mechanics Journal of Vibration and Acoustics 119 (1997) 374–389.
[8] A. Pica, R.D. Wood, E. Hinton, Finite element analysis of geometrically nonlinear plate behavior using a Mindlin formulation, Computers and Structures 11 (1980) 203–215.
[9] H.U. Akay, Dynamic large deflection analysis of plates using mixed finite elements, Computers & Structures 11 (1980) 1–11.
[10] J.N. Reddy, Geometrically nonlinear transient analysis of laminated composite plates, American Institute of Aeronautics and Astronautics Journal 21 (4) (1983) 621–629.
[11] H.S. Tsou, C.I. Tseng, Distributed modal identification and vibration control of continua: piezoelectric finite element formulation and analysis, Journal of Dynamic Systems, Measurement and Control 113 (1991) 500–505.
[12] S.K. Ha, C. Keilers, F.-K. Chang, Finite element analysis of composite structures containing distributed piezoelectric sensors and actuators, American Institute of Aeronautics and Astronautics Journal 30 (3) (1992) 772–780.
[13] W.S. Hwang, H.C. Park, Finite element modeling of piezoelectric sensors and actuators, American Institute of Aercnautics and Astronautics Journal 31 (1993) 930–937.
[14] P. Gaudenzi, K.J. Bathe, An iterative finite element procedure for the analysis of piezoelectric continua, Journal of Intelligent Material Systems and Structures. 6 (1995) 266–273.
[15] S.S. Rao, M. Sunar, Analysis of distributed thermopiezoelectric sensors and actuators in advanced intelligent structures, American Institute of Aeronautics and Astronautics Journal 31 (7) (1993) 1280–1286.
[16] K. Washizu, Variational Methods in Elasticity and Plasticity, 3rd Edition, Pergamon Press, New York, 1982.
[17] J.M. Yellin, I.Y. Shen, A self-sensing active constrained layer damping treatment for an Euler–Bernoulli beam, Journal of the Smart Material and Strutures 5 (1996) 628–637.